ACS OMEGA

Open Access

http://pubs.acs.org/journal/acsodf

Article

Boron Clusters Alter the Membrane Permeability of Dicationic Fluorescent DNA-Staining Dyes

Yuya Hirai,* Yoshimasa Makita,* Jun Asaoka, Yuka Aoyagi, Akihiro Nomoto, Hideyuki Okamura, and Shin-ichi Fujiwara

Cite This: *ACS Omega* 2023, 8, 35321−35327

Read Online

ACCESS | Metrics & More | Article Recommendations | Supporting Information

ABSTRACT: Membrane-permeable fluorescent dyes that stain DNA are useful reagents for microscopic imaging, as they can be introduced into living cells to label DNA. However, the number of these dyes, such as Hoechst 33342, is limited. Here, we show that the icosahedral dodecaborate $B_{12}Br_{12}^{2-}$, a superchaotropic carrier that delivers different types of molecules into cells, functions as an excellent carrier for membrane-impermeable fluorescent dyes. Propidium iodide (PI) and 4′,6-diamidino-2-phenylindole (DAPI), dicationic membrane-impermeable fluorescent dyes that stain DNA, can permeate cell membranes in the presence of boron clusters. Methyl green (MG), a dicationic dye used in the histological and fluorescent staining of DNA, permeated cell membranes in the presence of boron clusters. In contrast, monocationic membrane-permeable fluorescent dyes, such as acridine orange and pyronin Y, exhibited reduced fluorescence in cells in the presence of boron clusters. Boron clusters do not quench dicationic fluorescent dyes in water in vitro but have quenching effects on monocationic fluorescent dyes. We have demonstrated that the addition of $B_{12}Br_{12}^{2-}$ to impermeable dicationic fluorescent DNA-staining dyes, such as DAPI, PI, and MG, which have been widely used for numerous years, imparts membrane permeability to introduce these dyes into living cells.

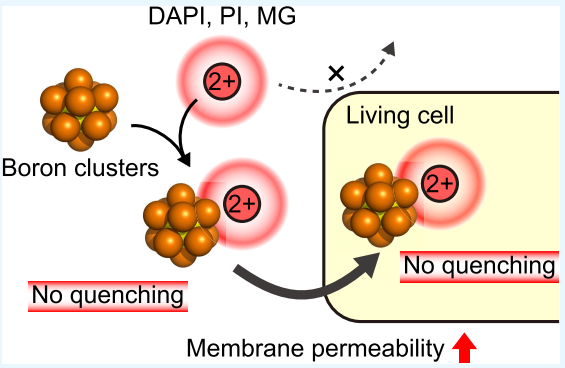

INTRODUCTION

Boron-containing compounds are widely used as pharmaceuticals.[1,2] Among them, boron clusters have recently drawn considerable attention owing to significant discoveries in their physicochemical properties.[3−7] Nau et al. particularly focused on icosahedral dodecaborates $B_{12}X_{12}^{2-}$ (X = H, Cl, Br, I), with particular emphasis on $B_{12}Br_{12}^{2-}$ (Figure 1A), an effective carrier of cationic and neutral small molecules.[5] $B_{12}Br_{12}^{2-}$ exhibits novel membrane permeability, characterized by a superchaotropic nature encompassing both high hydrophilicity[8,9] and lipophilicity.[10] Additionally, the chemical inertness of $B_{12}X_{12}^{2-}$ under physiological conditions has drawn interest in the exploration of new research avenues utilizing the superchaotropic properties of boron clusters.[4] Hence, attention has been paid to exploring the influence of boron cluster ions on a relatively wide variety of unexplored molecules.

The numerous fluorescent dyes used for DNA-staining have been extensively applied in both biological research and clinical diagnosis. These dyes play a crucial role in the study of intricate nuclear and chromosomal structures, facilitating contrasting staining of tissues and cells and the analysis of various cell cycle parameters.[11] However, simply increasing the lipophilicity of the dye to facilitate membrane permeation hinders the dissolution of organic-based dyes in water, causing precipitation and aggregation. In this state, the fluorescence is attenuated or extinguished, a phenomenon known as the aggregation-caused quenching (ACQ) effect.[12]

RESULTS AND DISCUSSION

We initially utilized a dicationic fluorescent DNA-staining dye of 4′,6-diamidino-2-phenylindole (DAPI) (Figure 1B),[13] a fluorescent DNA-staining dye that requires a significantly high concentration for effective introduction into living cells owing to its low membrane permeability.[14,15] To examine whether $B_{12}Br_{12}^{2-}$ facilitates the entry of DAPI into living cells, we compared the fluorescence intensity of DAPI at the final concentration of 10 μM with and without $B_{12}Br_{12}^{2-}$ in the live HeLa cells. As shown in Figure 2A, the DAPI fluorescence signal was stronger in the presence of $B_{12}Br_{12}^{2-}$ than it was in the absence of $B_{12}Br_{12}^{2-}$ (Figure 2A). Subsequently, we examined whether $B_{12}Br_{12}^{2-}$ allowed for the introduction of another dicationic membrane-impermeable dye, propidium iodide (PI)[16,17] (Figure 1C), into the living cells. PI was not

Received: July 17, 2023
Accepted: September 7, 2023
Published: September 14, 2023

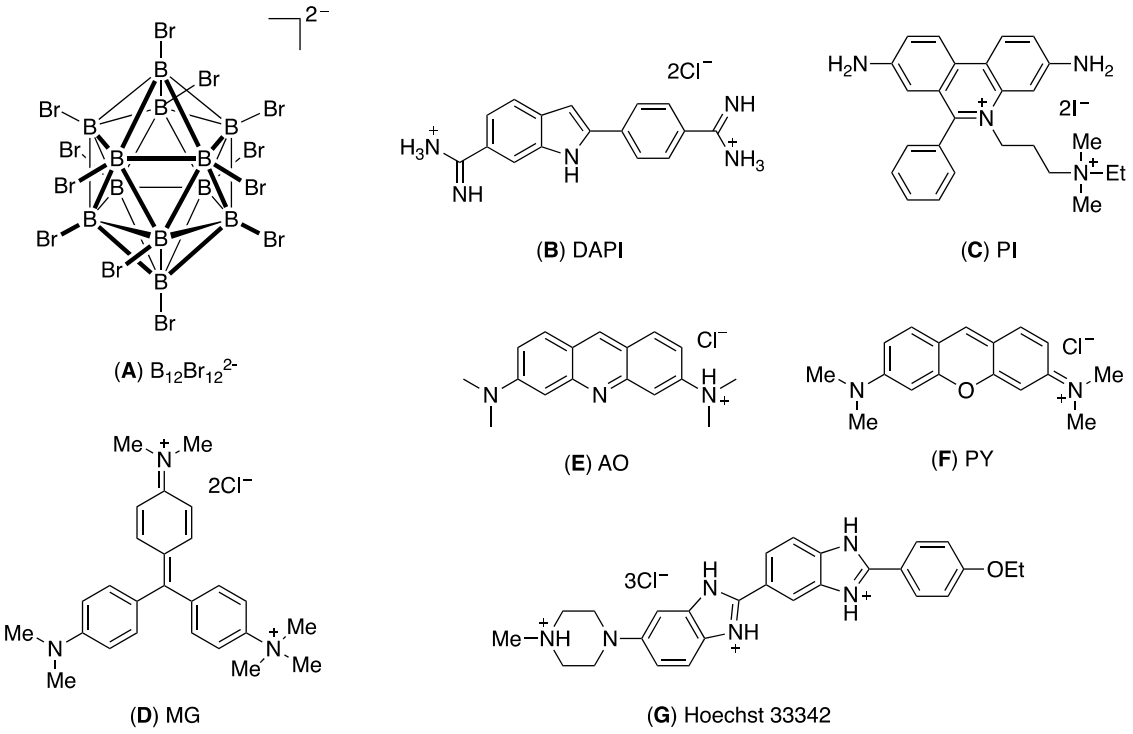

Figure 1. Structure of a boron cluster of $B_{12}Br_{12}^{2-}$ and fluorescent DNA-staining dyes.

introduced into live HeLa cells at a final concentration of 20 μM. However, it was successfully introduced into live HeLa cells containing $B_{12}Br_{12}^{2-}$ (Figures 2A and S1). Similar results were obtained in another cultured U-2 OS cell line (Figure 2B). These results show that $B_{12}Br_{12}^{2-}$ facilitated the entry of DAPI and PI into living cells.

This ability of $B_{12}Br_{12}^{2-}$ as a membrane carrier could also be applied to methyl green (MG) (Figure 1D), a triphenylmethane-based dicationic dye that has been widely employed for the nuclear staining of tissue sections in histological staining. Recently, diluted MG at physiological pH has been identified as a potential substitute for fluorescent staining of nonviable cells, presenting an alternative to currently utilized near-infrared dyes.[18] The advantage of using MG lies in its fluorescence property; its maximum excitation wavelength is at 633 nm, and its maximum emission wavelength is at 677 nm. This means that by using MG, nuclei can be labeled and detected in a Cy5 channel without using the three conventional channels: DAPI/blue, FITC/green, and TRITC/red. Similar to previous results, when cells were stained with MG and DAPI after fixation and permeabilization, MG was excited using a 639 nm laser, and its signal overlapped with that of DAPI (Figure 3A). The introduction of MG alone into living cells at a final concentration of 20 μM was difficult (Figure 3B). However, in the presence of $B_{12}Br_{12}^{2-}$, MG was introduced into living cells (Figure 3B). Noteworthily, there are two types of MG: one with the addition of $ZnCl_2$ and the other without it. In our experimental system, we confirmed that both reagents can effectively introduce MG into living cells (Figure S2). These results suggest that MG is a candidate fluorescent DNA-staining dye prior to fixation using $B_{12}Br_{12}^{2-}$.

Subsequently, we investigated the effects of $B_{12}Br_{12}^{2-}$ addition on the membrane permeability of known membrane-permeable monocationic fluorescent dyes, such as acridine orange (AO)[19,20] (Figure 1E) and pyronin Y (PY)[21] (Figure 1F), in living cells. Both AO and PY were introduced into living cells at a final concentration of 20 μM (Figure 4A). In contrast to those of DAPI, PI, and MG, the intracellular fluorescence intensities of both AO and PY were reduced in the presence of $B_{12}Br_{12}^{2-}$ (Figure 4A). Conversely, another membrane-permeable tricationic fluorescent DNA-staining dye, Hoechst 33342[14,22] (Figure 1G), did not show obvious differences in its fluorescence intensity at the final concentration of 0.2 or 2 μM in the absence and presence of $B_{12}Br_{12}^{2-}$ (Figure S3).

To investigate the variations in intracellular fluorescence intensity caused by differences in these fluorescent DNA-staining dyes, we measured the changes in fluorescence intensity resulting from the addition of the fluorescent DNA-staining dyes and $B_{12}Br_{12}^{2-}$ under in vitro conditions (Figure 5). In the case of DAPI, which is a dicationic dye, the fluorescence intensity did not change even in the presence of $B_{12}Br_{12}^{2-}$ (Figure 5A). This result supports the ability of $B_{12}Br_{12}^{2-}$ as a membrane carrier for DAPI because $B_{12}Br_{12}^{2-}$ does not affect the fluorescence intensity of DAPI. Unfortunately, we were unable to examine the change in the fluorescence intensities of the other dicationic dyes, PI and MG, because their fluorescence intensities were too low to be measured in our experimental system. On the contrary, the fluorescence intensities of AO and PY, both of which are monocationic dyes, decreased in the presence of $B_{12}Br_{12}^{2-}$ (Figure 5B,D). These results suggest that $B_{12}Br_{12}^{2-}$ functions as a quencher of AO and PY. In contrast, in the acetonitrile solvent, $B_{12}Br_{12}^{2-}$ did not show quenching for AO (Figure 5C). From these observations, we believe that in an aqueous solvent and probably also in the cells, $B_{12}Br_{12}^{2-}$ and two monocationic dyes aggregate through the superchaotropic effect, demonstrating the ACQ effect. Alternatively, the lack of fluorescence exhibited by AO and PY within the cells could be attributed to the inability of the dyes to penetrate the cellular

https://doi.org/10.1021/acsomega.3c05156
ACS Omega 2023, 8, 35321−35327

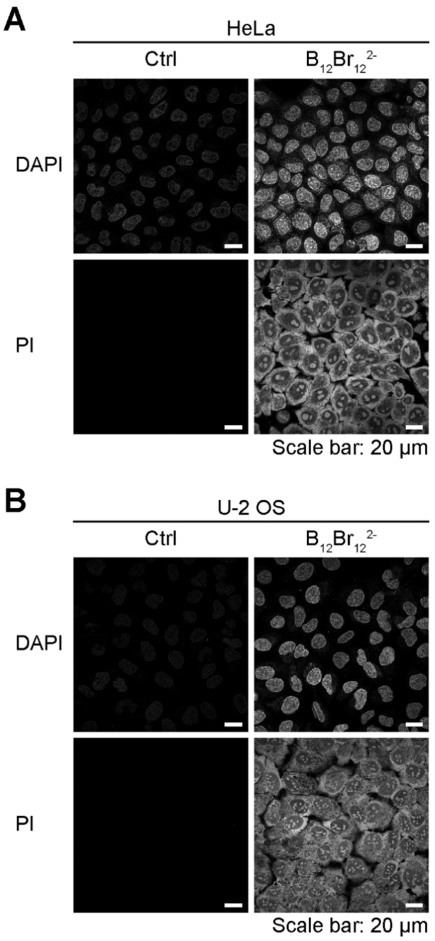

Figure 2. Effects of $B_{12}Br_{12}^{2-}$ as membrane carriers on DAPI and PI. DAPI or PI was introduced into the HeLa (A) or U-2 OS (B) cells in the absence or presence of $B_{12}Br_{12}^{2-}$, and these cells were observed by confocal fluorescence microscopy.

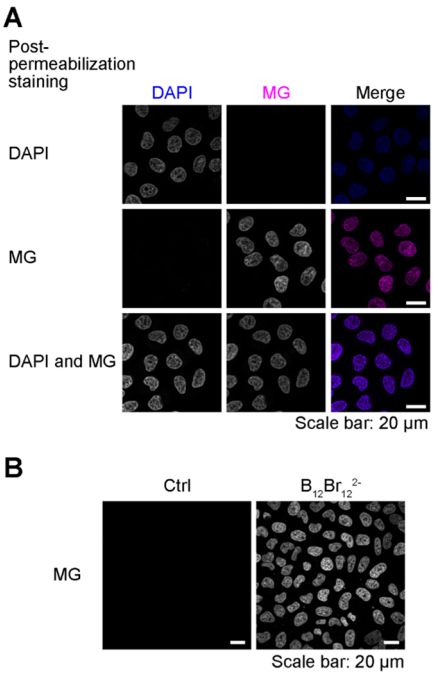

Figure 3. Effects of $B_{12}Br_{12}^{2-}$ as a membrane carrier on MG. (A) The fluorescence images of DAPI and MG on the postpermeabilized HeLa cells. The permeabilized HeLa cells were stained by DAPI (upper), MG (middle), or both DAPI and MG (lower); these cells were observed by confocal fluorescence microscopy. (B) MG was introduced into the HeLa cells in the absence or presence of $B_{12}Br_{12}^{2-}$, and these cells were observed by confocal fluorescence microscopy.

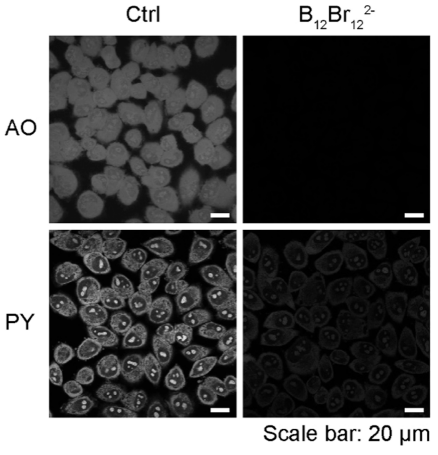

Figure 4. Effects of $B_{12}Br_{12}^{2-}$ as a membrane carrier on AO and PY. AO or PY were introduced into the HeLa cells in the absence or presence of $B_{12}Br_{12}^{2-}$, and these cells were observed by confocal fluorescence microscopy.

environment because of the aggregation caused by $B_{12}Br_{12}^{2-}$. In the case of Hoechst 33342, a tricationic dye, the fluorescence intensity decreased in the presence of $B_{12}Br_{12}^{2-}$ similar to those of monocationic dyes AO and PY (Figure 5E). However, there was no obvious change in the intracellular fluorescence intensity of Hoechst 33342 in the presence of $B_{12}Br_{12}^{2-}$ (Figure S2). Note that the introduction of Hoechst 33342 into the cells at the final concentrations of 20 μM, where Hoechst 33342 concentrations are toxic to cells,[23] induces cell death in the absence of $B_{12}Br_{12}^{2-}$, whereas its introduction in the presence of $B_{12}Br_{12}^{2-}$ was not lethal compared to the absence of $B_{12}Br_{12}^{2-}$ (Figure S3). To investigate changes in dye toxicity due to complex formation with $B_{12}Br_{12}^{2-}$, we measured the cytotoxicity of each dye with and without the $B_{12}Br_{12}^{2-}$. As a result of verifying the cytotoxicity of $B_{12}Br_{12}^{2-}$ itself, $B_{12}Br_{12}^{2-}$ had no significant cytotoxicity up to 150 μM (Figure 6A). Although DAPI alone did not show significant cytotoxicity, the cytotoxicity of DAPI was significantly increased in the presence of $B_{12}Br_{12}^{2-}$ (Figure 6B), supporting our finding that $B_{12}Br_{12}^{2-}$ increased the cell membrane permeability of DAPI (Figure 2). Although the cytotoxicity of PI was unchanged in the presence of $B_{12}Br_{12}^{2-}$ (Figure 6C), the cytotoxicity of MG was increased by the presence of $B_{12}Br_{12}^{2-}$ compared to MG alone (Figure 6D). AO exhibited cytotoxicity regardless of the presence of $B_{12}Br_{12}^{2-}$, whereas the presence of $B_{12}Br_{12}^{2-}$ did not alter the cytotoxicity of AO (Figure 6E). This result directs our initial hypothesis that the reduced fluorescence intensity of AO in the cells in the presence of $B_{12}Br_{12}^{2-}$ (Figure 4A) is due to the fact that AO is introduced into the cells in the presence of $B_{12}Br_{12}^{2-}$ but is quenched by the ACQ effect. Although PY alone also exhibited cytotoxicity, the presence of $B_{12}Br_{12}^{2-}$ did not change its cytotoxicity (Figure 6F). No significant difference in cytotoxicity between untreated and PY treatment in the presence of $B_{12}Br_{12}^{2-}$ was observed in the present experiment (Figure 6F). Hoechst 33342 was cytotoxic both alone and in

https://doi.org/10.1021/acsomega.3c05156
ACS Omega 2023, 8, 35321−35327

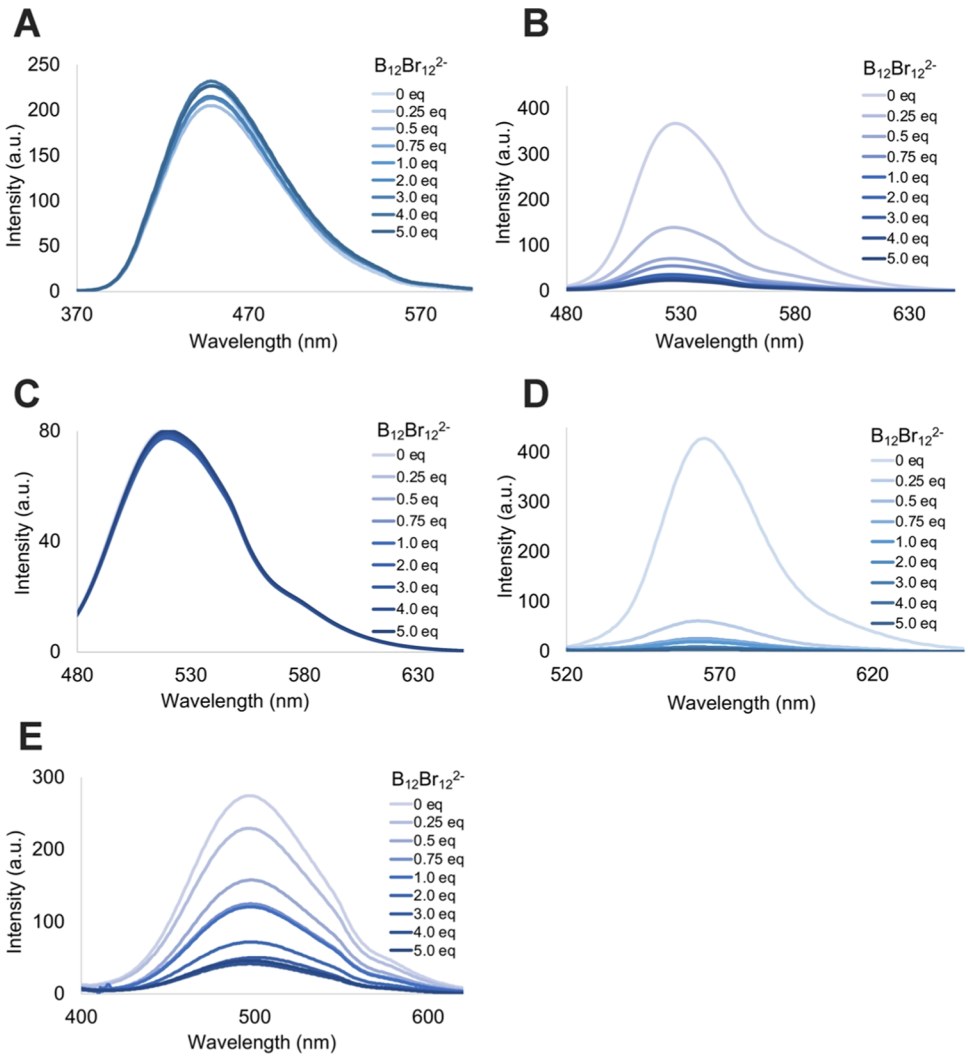

Figure 5. Fluorescence spectra of dyes with $B_{12}Br_{12}^{2-}$. (A) DAPI (2.0 μM, λ exciton = 358 nm) in H_2O. (B) AO (2.0 μM, λ_{exc} = 460 nm) in H_2O. (C) AO (2.0 μM, λ_{exc} = 460 nm) in CH_3CN. (D) PY (2.0 μM, λ_{exc} = 510 nm) in H_2O. (E) Hoechst 33342 (2.0 μM, λ_{exc} = 348 nm) in H_2O.

the presence of $B_{12}Br_{12}^{2-}$, and its cytotoxicity was reduced by the presence of $B_{12}Br_{12}^{2-}$ (Figure 6G). This result is consistent with the microscopic observations (Figure S3). One possible explanation for the reduced cytotoxicity of Hoechst 33342 due to the presence of $B_{12}Br_{12}^{2-}$ is that the binding mode to DNA was altered by complexing with $B_{12}Br_{12}^{2-}$. However, further analyses are required to elucidate the effects of $B_{12}Br_{12}^{2-}$ on the dye.

In conclusion, we demonstrated that the addition of $B_{12}Br_{12}^{2-}$ to impermeable dicationic fluorescent DNA-staining dyes DAPI, PI, and MG imparts membrane permeability to introduce these dyes into living cells without the ACQ effect.

MATERIALS AND METHODS

$B_{12}Br_{12}^{2-}$. $Cs_2B_{12}Br_{12}$ was employed as $B_{12}Br_{12}^{2-}$, which was synthesized from $Cs_2B_{12}H_{12}$ (55−1800; Strem Chemicals, Inc.) using the following procedure.[24]

Cells. HeLa S3 cells and U-2 osteosarcoma (OS) cells were cultured in low-glucose (1.0 g/L) Dulbecco's modified Eagle medium (DMEM) (041-29775; Wako or 08456-65; Nacalai Tesque) supplemented with 10% fetal bovine serum (FBS).

Confocal Microscopy. The cells were cultured on coverslips in 24-well plates. First, 10 μM 4′,6′-diamidino-2-phenylindole (DAPI) (D5888; TCI), 0.2, 2, or 20 μM Hoechst 33342 (H3570; Invitrogen), 20 μM propidium iodide (PI) (P4864; Sigma), 20 μM methyl green (MG) (136-05352; Wako, or M0498; TCI), 20 μM acridine orange (AO) (A3396; TCI) or 20 μM pyronin Y (PY) (164-11581; Wako), and 100 μM $Cs_2B_{12}Br_{12}$ were mixed in serum-free DMEM and incubated for 15 min at room temperature (RT). After the cells were washed twice with phosphate-buffered saline (PBS), the complex mixtures were added and incubated for 2 h in a CO_2 incubator. The cells were then washed twice with PBS and fixed with 4% paraformaldehyde (PFA) for 10 min. After washing twice with PBS, the cells were mounted with mounting medium (Tris-based 90% glycerol) containing 2.5% 1,4-diazabicyclo[2.2.2]octane (DABCO) (D0134; TCI) (for DAPI, PI, and MG), 2.5% DABCO, and 0.5% *n*-propyl gallate (P3130; Sigma) (for AO and PY). For postpermeabilization staining, cultured cells were fixed with 4% PFA for 10 min. After washing twice with PBS, the cells were incubated with 1 μM DAPI, 5 μM MG, or both in PBS containing 0.5% Triton X-100 for 15 min. After washing twice, the cells were mounted on mounting media. The cells were observed under a laser scanning confocal microscope (LSM 700; Carl Zeiss AG) equipped with a Plan-Apochromat 63× objective lens

https://doi.org/10.1021/acsomega.3c05156
ACS Omega 2023, 8, 35321−35327

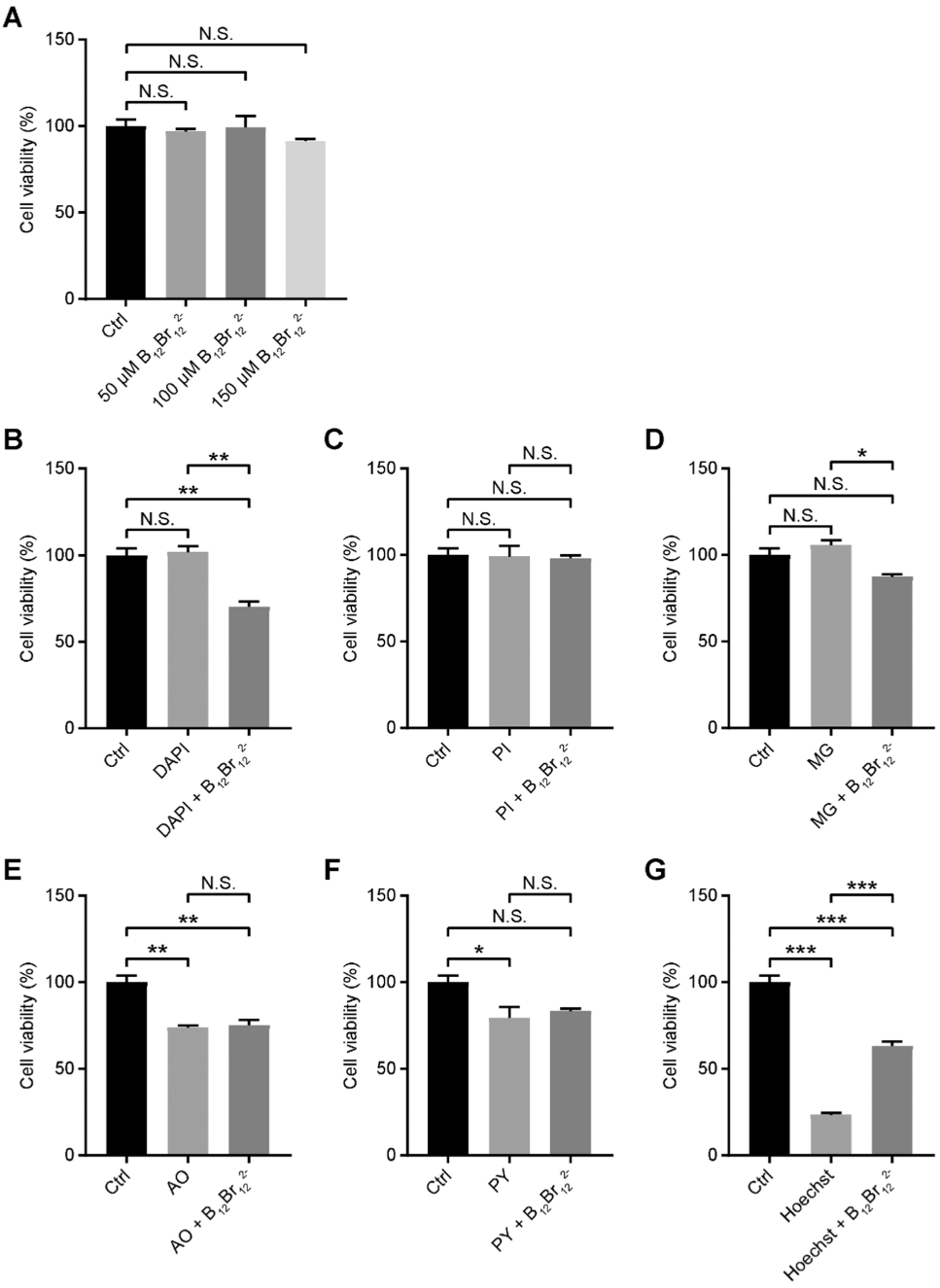

Figure 6. Cytotoxicity of dyes with the $B_{12}Br_{12}^{2-}$. (A) $B_{12}Br_{12}^{2-}$ was introduced into the U-2 OS cells at the final concentration of 50, 100, or 150 μM, and the cell viability was measured. (B–G) DAPI (B), PI (C), MG (D), AO (E), PY (F), and Hoechst 33342 (G) were introduced into the U-2 OS cells and each cell viability was measured. Values were normalized to the control cells (100%). Data are mean ± standard error of the mean (SEM) (n = 3). Statistical significance was calculated with one-way analysis of variance (ANOVA), followed by Tukey's multiple comparisons test. *: $P < 0.05$, **: $P < 0.01$, ***: $P < 0.001$, N.S.: not significant.

(numerical aperture = 1.4). The following lasers were used to excite the fluorescent dyes in our experiments: 405 nm for DAPI and Hoechst 33342, 488 nm for AO, 555 nm for PI and PY, and 639 nm for MG.

Fluorescence Measurement. The 100 μM $Cs_2B_{12}Br_{12}$, DAPI, AO, PY, and Hoechst 33342 in H_2O and the 100 μM $Cs_2B_{12}Br_{12}$ in CH_3CN solutions were prepared as stock solutions. Further, 2.0 μM DAPI/$Cs_2B_{12}Br_{12}$ = 1:1 in H_2O solution was prepared by adding 60 μL of DAPI and 60 μL of a $Cs_2B_{12}Br_{12}$ stock solution into 2880 μL of H_2O in a cuvette. The fluorescence spectra were obtained using a JASCO FP-6300 instrument at room temperature. The slit width was 5 nm for both excitation and emission, a resolution of 1 nm. All spectra were corrected for the blank. The excitation wavelengths of DAPI, AO, PY, and Hoechst 33342 were 358, 460, 510, and 348 nm, respectively.

Cell Viability Assay. U-2 OS cells were cultured in a 96-well plate. First, 50, 100, or 150 μM $Cs_2B_{12}Br_{12}$ was mixed in serum-free DMEM and incubated for 15 min at room temperature (RT). Alternatively, 10 μM DAPI, 20 μM PI, 20 μM MG, 20 μM AO, 20 μM PY, or 20 μM Hoechst 33342 was mixed in serum-free DMEM in the presence or absence of 100 μM $Cs_2B_{12}Br_{12}$ and incubated for 15 min at room temperature (RT). After the cells were washed twice with PBS,

https://doi.org/10.1021/acsomega.3c05156
ACS Omega 2023, 8, 35321−35327

the complex mixtures were added and incubated for 2 h in a CO_2 incubator. After washing the cells twice with PBS, the cell viability was determined by Cell Counting Kit-8 (CK04; Dojindo) according to the manufacturer's instructions. The absorbance at 450 and 620 nm were measured with a plate reader (Multiskan FC; Thermo Fisher Scientific), and the data were normalized to the value of untreated cells.

■ ASSOCIATED CONTENT

Supporting Information

The Supporting Information is available free of charge at https://pubs.acs.org/doi/10.1021/acsomega.3c05156.

Effects of $B_{12}Br_{12}^{2-}$ as membrane carriers on PI (Figure S1); effects of zinc ions in MG as cargos of $B_{12}Br_{12}^{2-}$ (Figure S2); and effects of the $B_{12}Br_{12}^{2-}$ anions as membrane carriers on Hoechst 33342 (Figure S3) (PDF)

■ AUTHOR INFORMATION

Corresponding Authors

Yuya Hirai − *Department of Biology, Osaka Dental University, Hirakata, Osaka 573-1121, Japan;* orcid.org/0000-0001-8571-080X; Email: hirai-y@cc.osaka-dent.ac.jp

Yoshimasa Makita − *Department of Chemistry, Osaka Dental University, Hirakata, Osaka 573-1121, Japan;* orcid.org/0000-0003-4732-8145; Email: makita@cc.osaka-dent.ac.jp

Authors

Jun Asaoka − *Department of Applied Chemistry, Graduate School of Engineering, Osaka Metropolitan University, Sakai, Osaka 599-8531, Japan*

Yuka Aoyagi − *Department of Applied Chemistry, Graduate School of Engineering, Osaka Metropolitan University, Sakai, Osaka 599-8531, Japan*

Akihiro Nomoto − *Department of Applied Chemistry, Graduate School of Engineering, Osaka Metropolitan University, Sakai, Osaka 599-8531, Japan;* orcid.org/0000-0003-3427-2234

Hideyuki Okamura − *Department of Biology, Osaka Dental University, Hirakata, Osaka 573-1121, Japan*

Shin-ichi Fujiwara − *Department of Chemistry, Osaka Dental University, Hirakata, Osaka 573-1121, Japan*

Complete contact information is available at: https://pubs.acs.org/10.1021/acsomega.3c05156

Author Contributions

Y.H. and Y.M. conceptualized and designed the study. Y.H., Y.M., J.A., and Y.A. performed the experiments. Y.H. and Y.M. analyzed the data and interpreted the data. Y.H. and Y.M. wrote the initial draft of the manuscript, and all authors revised the manuscript.

Notes

The authors declare no competing financial interest.

■ ACKNOWLEDGMENTS

This work was supported in part by JSPS KAKENHI, Grant Numbers JP23K06574 (Y.H.) and JP18K09629 (Y.M.).

■ ABBREVIATIONS

DAPI, 4′,6′-diamidino-2-phenylindole; PI, propidium iodide; MG, methyl green; AO, acridine orange; PY, pyronin Y

■ REFERENCES

(1) Soloway, A. H.; Tjarks, W.; Barnum, B. A.; Rong, F.-G.; Barth, R. F.; Codogni, I. M.; Wilson, J. G. The chemistry of neutron capture therapy. *Chem. Rev.* **1998**, *98*, 1515−1562.

(2) Gabel, D. Boron clusters in medicinal chemistry: perspectives and problems. *Pure Appl. Chem.* **2015**, *87*, 173−179.

(3) Assaf, K. I.; Ural, M. S.; Pan, F.; Georgiev, T.; Simova, S.; Rissanen, K.; Gabel, D.; Nau, W. M. Water structure recovery in chaotropic anion recognition: high-affinity binding of dodecaborate clusters to γ-cyclodextrin. *Angew. Chem., Int. Ed.* **2015**, *54*, 6852−6856.

(4) Assaf, K. I.; Nau, W. M. The chaotropic effect as an assembly motif in chemistry. *Angew. Chem., Int. Ed.* **2018**, *57*, 13968−13981.

(5) Barba-Bon, A.; Salluce, G.; Lostalé-Seijo, I.; Assaf, K. I.; Hennig, A.; Montenegro, J.; Nau, W. M. Boron clusters as broadband membrane carriers. *Nature* **2022**, *603*, 637−642.

(6) Chen, Y.; Barba-Bon, A.; Grüner, B.; Winterhalter, M.; Aksoyoglu, M. A.; Pangeni, S.; Ashjari, M.; Brix, K.; Salluce, G.; Folgar-Cameán, Y.; Montenegro, J.; Nau, W. M. Metallacarborane cluster anions of the cobalt bisdicarbollide-type as chaotropic carriers for transmembrane and intracellular delivery of cationic peptides. *J. Am. Chem. Soc.* **2023**, *145*, 13089−13098.

(7) Cebula, J.; Fink, K.; Boratyński, J.; Goszczyński, T. M. Supramolecular chemistry of anionic boron clusters and its applications in biology. *Coord. Chem. Rev.* **2023**, *477*, No. 214940.

(8) Karki, K.; Gabel, D.; Roccatano, D. Structure and dynamics of dodecaborate clusters in water. *Inorg. Chem.* **2012**, *51*, 4894−4896.

(9) Hollow, S. E.; Johnstone, T. C. Encapsulation of closo-dodecaiododododecaborate in 2-hydroxypropyl-γ-cyclodextrin prevents hemolysis. *Chem. Commun.* **2022**, *58*, 2375−2378.

(10) Plesek, J. Potential applications of the boron cluster compounds. *Chem. Rev.* **1992**, *92*, 269−278.

(11) Klonisch, T.; Wark, L.; Hombach-Klonisch, S.; Mai, S. Nuclear imaging in three dimensions: a unique tool in cancer research. *Ann. Anat.* **2010**, *192*, 292−301.

(12) Mei, J.; Leung, N. L. C.; Kwok, R. T. K.; Lam, J. W. Y.; Tang, B. Z. Aggregation-induced emission: together we shine, united we soar! *Chem. Rev.* **2015**, *115*, 11718−11940.

(13) Kapuscinski, J. DAPI: a DNA-specific fluorescent probe. *Biotechnol. Histochem.* **1995**, *70*, 220−233.

(14) Haraguchi, T.; Ding, D.-Q.; Yamamoto, A.; Kaneda, T.; Koujin, T.; Hiraoka, Y. Multiple-color fluorescence imaging of chromosomes and microtubules in living cells. *Cell Struct. Funct.* **1999**, *24*, 291−298.

(15) Zink, D.; Sadoni, N.; Stelzer, E. Visualizing chromatin and chromosomes in living cells. *Methods* **2003**, *29*, 42−50.

(16) Krishan, A. Rapid flow cytofluorometric analysis of mammalian cell cycle by propidium iodide staining. *J. Cell Biol.* **1975**, *66*, 188−193.

(17) Hudson, B.; Upholt, W. B.; Devinny, J.; Vinograd, J. The use of an ethidium analogue in the dye-buoyant density procedure for the isolation of closed circular DNA: the variation of the superhelix density of mitochondrial DNA. *Proc. Natl. Acad. Sci. U.S.A.* **1969**, *62*, 813−820.

(18) Prieto, D.; Aparicio, G.; Morande, P. E.; Zolessi, F. R. A fast, low cost, and highly efficient fluorescent DNA labeling method using methyl green. *Histochem. Cell Biol.* **2014**, *142*, 335−345.

(19) Vinegar, R. Metachromatic differential fluorochroming of living and dead ascites tumor cells with acridine orange. *Cancer Res.* **1956**, *16*, 900−906.

(20) Nicolini, C.; Belmont, A.; Parodi, S.; Lessin, S.; Abraham, S. Mass action and acridine orange staining: static and flow cytofluorometry. *J. Histochem. Cytochem.* **1979**, *27*, 102−113.

(21) Shapiro, H. M. Flow cytometric estimation of DNA and RNA content in intact cells stained with Hoechst 33342 and Pyronin Y. *Cytometry* **1981**, *2*, 143−150.

(22) Arndt-Jovin, D. J.; Jovin, T. M. Analysis and sorting of living cells according to deoxyribonucleic acid content. *J. Histochem. Cytochem.* **1977**, *25*, 585−589.

(23) Durand, R. E.; Olive, P. L. Cytotoxicity, mutagenicity and DNA damage by Hoechst 33342. *J. Histochem. Cytochem.* **1982**, *30*, 111−116.
(24) Tiritiris, I.; Schleid, T. Die kristallstrukturen der dicaesium-dodekahalogeno-closo-dodekaborate Cs2[B12 × 12] (X = Cl, Br, I) und ihrer hydrate. *Z. Anorg. Allg. Chem.* **2004**, *630*, 1555−1563.

https://doi.org/10.1021/acsomega.3c05156
ACS Omega 2023, 8, 35321−35327